01 May 1975

Binary Nucleation. I. Theory Applied to Water-Ethanol Vapors

Gerald Wilemski
Missouri University of Science and Technology, wilemski@mst.edu

Recommended Citation

G. Wilemski, "Binary Nucleation. I. Theory Applied to Water-Ethanol Vapors," *Journal of Chemical Physics*, vol. 62, no. 9, pp. 3763-3771, American Institute of Physics (AIP), May 1975.
The definitive version is available at https://doi.org/10.1063/1.430945

Binary nucleation. I. Theory applied to water–ethanol vapors*

Gerald Wilemski†

Department of Engineering and Applied Science, Yale University, New Haven, Connecticut 06520
(Received 27 December 1974)

A quantitative study of nucleation in vapor mixtures of ethanol and water near 273 °C is presented. First, Reiss' theory of binary nucleation is reexamined. The theory is modified slightly in order to yield the proper limit for homogeneous nucleation in a one-component system. Moreover, a corrected expression for the equilibrium concentration of mixed clusters is derived. Calculations of the critical vapor activities needed to produce a visible condensate are presented and compared with the results of Flood's cloud chamber experiments. The agreement is only fair, but qualitative accord is found.

I. INTRODUCTION

Over 20 years ago, Reiss[1] published a theory of nucleation in two-component systems (binary or heteromolecular nucleation) which has served as the basis for the theoretical prediction of steady state nucleation rates in binary vapor mixtures.[2–5] Although this theory has greatly enhanced our understanding of nucleation in binary systems, it has received little, if any, quantitative comparison with experiment. Before making comparisons, however, two aspects of the theory are in need of further clarification.

It will be seen that under certain limiting conditions, which can be important in evaluating experimental data, Reiss' theory gives qualitatively unsatisfactory predictions. One defect can sometimes be eliminated, as will be shown, by modifying slightly the definition of the nucleation rate in a two-component system. Correction of the other defect involves reconsidering the thermodynamics of mixed cluster formation in a fashion analogous to that of Dunning[6] and Blander and Katz[7] for pure clusters.

II. OUTLINE OF REISS' THEORY

The vapor consists of a mixture of the condensable species 1 and 2 out of which clusters of composition (n_1, n_2) are formed. Here n_i is the number of molecules of Species i in the cluster. Reiss considered a two dimensional lattice in which n_1 served as abscissa and n_2 as ordinate. Points on the lattice thus represent different cluster compositions. Clusters are assumed to grow and decay by the gain and loss of single molecules of either species. A nucleation current vector I can be defined whose components $I_1(n_1, n_2)$ and $I_2(n_1, n_2)$ are the net rates at which clusters of composition (n_1, n_2) become clusters of composition (n_1+1, n_2) and (n_1, n_2+1), respectively. When the n_i are treated as continuous variables, the I_i are given as

$$I_i(n_1, n_2) = c(n_1, n_2)\mathcal{O}(n_1, n_2)\beta_i \frac{\partial(f/c)}{\partial n_i} . \tag{2.1}$$

Here, $f(n_1, n_2, t)$ is the concentration of clusters of composition (n_1, n_2) present at time t; $c(n_1, n_2)$ is the equilibrium concentration of these clusters; $\mathcal{O}$ is their surface area; and β_i is the impingement frequency/area of Species i on the cluster surface and is usually taken as

$$\beta_i = p_i/(2\pi m_i kT)^{1/2}, \tag{2.2}$$

where p_i is the pressure of Species i in the vapor, m_i is the molecular mass, k is Boltzmann's constant, and T is the temperature. For c, Reiss gave the following expression:

$$c(n_1, n_2) = (c_1 + c_2)e^{-w(n_1, n_2)/kT}, \tag{2.3}$$

where c_i is the monomer concentration of Species i in the vapor, and $w(n_1, n_2)$ is supposed to be the reversible work of formation of the cluster (n_1, n_2). For vapor–liquid nucleation, w has been given[1,2] as

$$w(n_1, n_2) = n_1\Delta\mu_1(x) + n_2\Delta\mu_2(x) + \mathcal{O}(n_1, n_2)\sigma(x), \tag{2.4}$$

with

$$x = n_2/(n_1 + n_2) . \tag{2.5}$$

The mole fraction of Species 2 is denoted by x. In Eq. (2.4), $\Delta\mu_i$ is the chemical potential difference for a molecule of Species i in a solution of composition x and in the vapor at a pressure p_i. If the gases can be considered ideal and small pV terms are neglected,

$$\Delta\mu_i = -kT\ln[p_i/p_i^s(x)], \tag{2.6}$$

where $p_i^s(x)$ is the equilibrium vapor pressure of Species i at T over an infinite plane surface of solution of bulk composition x. Finally, $\sigma(x)$ is the surface tension and is a function of composition as well as temperature.

The requirement that for some composition (n_1^*, n_2^*) the chemical potentials of molecules in the cluster equal those in the vapor leads to the Gibbs–Thomson equations for binary drops:

$$0 = \left(\frac{\partial w}{\partial n_1}\right)_{n_2} = \Delta\mu_1 + \frac{2\sigma v_1}{r} - \frac{3xv}{r}\frac{d\sigma}{dx}, \tag{2.7a}$$

$$0 = \left(\frac{\partial w}{\partial n_2}\right)_{n_1} = \Delta\mu_2 + \frac{2\sigma v_2}{r} + \frac{3(1-x)v}{r}\frac{d\sigma}{dx}, \tag{2.7b}$$

where

$$v = (1-x)v_1 + xv_2 . \tag{2.8}$$

The quantity v_i is the partial molecular volume of Species i in solution, and v is the average molecular volume of the solution. Both quantities are composition dependent.

The values n_1^* and n_2^* define the critical composition for which an unstable equilibrium exists for the droplet in the vapor. They also locate a saddle point on the free energy surface $w(n_1, n_2)$.[1,2] It is next assumed that the principal nucleation currents proceed through the "pass" in the free energy surface located about the saddle point. The principal objective of the theory is to calculate the

steady state nucleation current through this pass. This may be done in an approximate manner which is slightly more general than that of Reiss.

In the steady state there will exist "streamlines" on which the magnitude of the nucleation current vector I is constant. These streamlines can be used to characterize a set of curvilinear coordinates ξ_1 and ξ_2, in which ξ_2 designates particular streamlines and ξ_1 designates distance along a streamline. It should be safe to assume that the new coordinates are orthogonal, at least in some neighborhood of the principal nucleation current. Under this assumption the components of I in the two coordinate systems are related by the following equations:

$$g_i = h_i(\partial\xi_1/\partial n_1)I_1 + h_i(\partial\xi_2/\partial n_2)I_2\,, \quad i=1,\ 2\,. \tag{2.9}$$

The h_i are scale factors[8] for the new coordinates. It is next assumed, as Reiss did, that the principal nucleation currents arise near the origin (the monomer states) and that the component of I along the streamline, g_1, is essentially equal to the magnitude of I, i.e., that the component orthogonal to the streamline, g_2, is negligible all along the path. This should be a good approximation for paths in the vicinity of the saddle point. Expressed mathematically, the assumption that

$$g_2 = 0 \tag{2.10}$$

implies

$$g_1 = I(\xi_2)\,. \tag{2.11}$$

Now, after expressing I_1 and I_2 in terms of the new coordinates, Eqs. (2.9)–(2.11) can be reduced to

$$I(\xi_2)/[cD(\xi_1,\ \xi_2)] = -\partial(f/c)/\partial\xi_1\,, \tag{2.12}$$

where

$$D(\xi_1,\ \xi_2) = \beta_1\beta_2 \frac{\mathcal{O}h_1\left[\left(\frac{\partial\xi_1}{\partial n_1}\right)^2\left(\frac{\partial\xi_2}{\partial n_2}\right)^2 - \left(\frac{\partial\xi_1}{\partial n_1}\right)\left(\frac{\partial\xi_1}{\partial n_2}\right)\left(\frac{\partial\xi_2}{\partial n_1}\right)\left(\frac{\partial\xi_2}{\partial n_2}\right)\right]}{\left[\beta_1\left(\frac{\partial\xi_2}{\partial n_1}\right)^2 + \beta_2\left(\frac{\partial\xi_2}{\partial n_2}\right)^2\right]}\,. \tag{2.13}$$

Integrating Eq. (2.12) along any streamline which lies near the saddle point leads to the result

$$I(\xi_2) = \left(\int_0^\infty d\xi_1[cD(\xi_1,\ \xi_2)]^{-1}\right)^{-1}\,. \tag{2.14}$$

Reiss defines the over-all nucleation rate as

$$J_B = \int_{-\infty}^{\infty} I(\xi_2)d\xi_2\,, \tag{2.15}$$

which effectively sums all of the nonvanishing currents flowing through the pass. In the neighborhood of the saddle point, it is likely that the curvilinear coordinate system behaves like a Cartesian system. In this case, the following transformation will enable the saddle point integration to be performed:

$$\xi_1 = \xi_1^* + u_1\,, \tag{2.16a}$$

$$\xi_2 = u_2\,, \tag{2.16b}$$

where $\xi_2^* = 0$ by definition, and u_1 and u_2 arise from the rotation

$$n_1 - n_1^* = u_1\cos\phi - u_2\sin\phi\,, \tag{2.17a}$$

$$n_2 - n_2^* = u_1\sin\phi + u_2\cos\phi\,. \tag{2.17b}$$

The angle ϕ is the angle made by the axis of the pass with the n_1 axis of the original coordinate system, and it is further defined in Appendix B. The transformation into u_1 and u_2 permits the evaluation of $D(\xi_1,\ \xi_2)$ to be made at the saddle point. Equations (2.14) and (2.15) may also now be evaluated in the manner of Reiss, using the method of steepest descent. All of the results are, of course, identical to his, and they appear as

$$I(\xi_2) = D^*(p/2\pi kT)^{1/2}c(n_1^*,\ n_2^*)e^{-q\xi_2^2/(2kT)}\,, \tag{2.18}$$

and

$$J_B = D^*(p/q)^{1/2}c(n_1^*,\ n_2^*)\,, \tag{2.19}$$

where

$$D^* = \beta_1\beta_2\mathcal{O}^*/(\beta_1\sin^2\phi + \beta_2\cos^2\phi)\,, \tag{2.20}$$

$$p = -(\partial^2 w/\partial u_1^2)^*\,, \tag{2.21a}$$

$$q = (\partial^2 w/\partial u_2^2)^*\,. \tag{2.21b}$$

III. THE EQUILIBRIUM DISTRIBUTION

Under appropriate conditions, in vapors with components possessing an unfavorable free energy of mixing, only homogeneous nucleation of one component, say Species 1, should result. Yet, as pointed out by Katz,[9] because of Eqs. (2.3) and (2.19) the nucleation rate of pure clusters of Species 1 would still depend linearly on the *total* pressure of the vapor mixture.

The implication of this observation is that the pressure of the inert carrier gas should have an appreciable effect on the rate of homogeneous nucleation of the remaining condensable vapor. Such an effect is indeed found experimentally,[10] and it is usually attributed to the effects of nonisothermal nucleation.[11] However, the present theory, as formulated, does not include any of these effects, and it should reduce under the described conditions to the *isothermal* homogeneous nucleation of a vapor in an inert carrier gas. It is well known that the theory for this latter process does not include any significant dependence on the carrier gas pressure. This inconsistency may be eliminated by properly defining the free energy of a mixed cluster. Following the discussions of Dunning[6] and Blander and Katz,[7] a self-consistent expression for the equilibrium cluster concentration may be obtained.

For the existence of equilibrium between clusters of composition $(n_1,\ n_2)$ and the two monomeric species, the usual relationship among the chemical potential of the different species must be satisfied:

$$n_1\mu_1 + n_2\mu_2 = \mu(n_1,\ n_2)\,, \tag{3.1}$$

where μ_i is the chemical potential of Species i in the vapor, and $\mu(n_1,\ n_2)$ is the chemical potential of clusters of composition $(n_1,\ n_2)$. Provided that interactions between different clusters are small, the vapor may be considered as an ideal gas mixture. Then the chemical potentials have the form

$$\mu_i = \mu_i^0 + kT \ln c_i \tag{3.2}$$

and

$$\mu(n_1, n_2) = \mu^0(n_1, n_2) + kT \ln c(n_1, n_2). \tag{3.3}$$

The standard states have been taken as one per unit volume. Equations (3.1)–(3.3) give

$$c(n_1, n_2) = (c_1)^{n_1}(c_2)^{n_2} \times \exp\{-[\mu^0(n_1, n_2) - n_1\mu_1^0 - n_2\mu_2^0)]/kT\}. \tag{3.4}$$

When the vapor is in equilibrium with solution of bulk composition x, the concentration of Species i in the vapor is c_i^∞. Then

$$\mu_i^s(x) = \mu_i^0 + kT \ln c_i^\infty, \tag{3.5}$$

where $\mu_i^s(x)$ is the chemical potential of Species i in the solution. Equations (3.4) and (3.5) give

$$c(n_1, n_2) = \left(\frac{p_1}{p_1^s(x)}\right)^{n_1}\left(\frac{p_2}{p_2^s(x)}\right)^{n_2} \times \exp\{-[\mu^0(n_1, n_2) - n_1\mu_1^s - n_2\mu_2^s]/kT\}. \tag{3.6}$$

The quantity $\mu^0(n_1, n_2) - n_1\mu_1^s - n_2\mu_2^s$ can be interpreted as the change in free energy upon taking the appropriate n_1+n_2 molecules from a vapor in equilibrium with bulk solution of composition x and converting them into a cluster of composition (n_1, n_2) in the standard state of one per unit volume. By generalizing the statistical mechanical droplet theory[6] to include mixed drops, $\mu^0(n_1, n_2)$ can be related to the cluster partition function $Q(n_1, n_2)$. Thus,

$$\mu^0(n_1, n_2) = -kT \ln[Q(n_1, n_2)/V], \tag{3.7}$$

and

$$Q(n_1, n_2) = (h^{3(n_1+n_2)} n_1! n_2!)^{-1} \int e^{-H/kT} d\{q\} d\{p\}. \tag{3.8}$$

Here, H is the Hamiltonian function for the n_1+n_2 molecule cluster, and the integration is carried out with respect to all coordinates and momenta accessible to molecules in the cluster. Although, at present, Eq. (3.8) cannot in general be rigorously evaluated, it can be expressed formally as[6,12]

$$Q(n_1, n_2) = \frac{Q_{tr}Q_{rot}}{Q_{rep}} e^{-(n_1\mu_1^s + n_2\mu_2^s)/kT} e^{-\sigma S/kT}. \tag{3.9}$$

Here, Q_{tr} and Q_{rot} are the translational and rotational partition functions for the cluster, σS is the surface free energy of the cluster, and Q_{rep} is a correction partition function which, in principle, takes into account any inadequacies and inconsistencies in the assumed form of Eq. (3.9). Examples of these are (1) the fact that, if $Q_{rep} = 1$, Eq. (9) receives contributions from six too many degrees of freedom, and (2) the likely possibility that the rotational degrees of freedom are not separable. Another major task for Q_{rep} is to relate the configurational partition function of the cluster to the free energy of n_1+n_2 molecules in solution. Several phenomenological prescriptions for Q_{rep} exist for the analogous problem in homogeneous nucleation,[13] and these may be adapted for use here. Equations (3.6) and (3.9) give

$$c(n_1, n_2) = \frac{Q_{tr}Q_{rot}}{VQ_{rep}} e^{-w(n_1, n_2)/kT}, \tag{3.10}$$

and, for example, with Dunning's prescription,[14] Eq. (3.10) becomes

$$c(n_1, n_2) = \frac{4}{n^{1/3}v_f} e^{-w/kT}, \tag{3.11}$$

where $n = n_1 + n_2$, and v_f is the average free volume per molecule in the solution. Obviously, in order to recover Eq. (2.3), it is necessary to put

$$\frac{Q_{tr}Q_{rot}}{VQ_{rep}} = c_1 + c_2,$$

but in view of the nature of Q_{rep} it seems unjustifiable to introduce such a dependence on c_1+c_2, and it certainly violates the mass action law for chemical equilibria.

IV. HOMOGENEOUS NUCLEATION LIMIT

On the basis of physical considerations, it should be expected that a theory of nucleation in two-component systems should predict homogeneous nucleation of one component when either the equilibrium vapor pressure of one component becomes excessively large, i.e., there is a very unfavorable free energy of mixing, or the concentration of one species in the vapor becomes exceedingly small. For the former limiting condition, the improper behavior of the equilibrium distribution necessitated the additional thermodynamic considerations presented in the preceding section. It will now be seen that under both of these limiting conditions, Eq. (2.19) fails to yield homogeneous nucleation of one component.

Using $w(n_1, n_2)$ as defined in Eq. (2.4) along with Eqs. (2.5)–(2.8) the following general results are deduced in Appendix A:

(1) As $p_1 \to 0$ *or* $p_1^s(x) \to \infty (x \neq 1)$, $n_1^* \to 0$ and $x^* \to 1$. The critical cluster composition becomes pure in Species 2.

(2) As $p_2 \to 0$ *or* $p_2^s(x) \to \infty (x \neq 0)$, $n_1^* \to 0$ and $x^* \to 0$. The critical cluster composition becomes pure in Species 1.

On physical grounds, these results can not be expected to change when different choices for w are made (implying different choices for Q_{rep}). In Appendix B, the limiting behavior of Eq. (2.19) is examined in detail. It may be shown that, in general, as $x^* \to 0$ or 1,

$$J_B \approx \left(\frac{2\pi kT}{q}\right)^{1/2} J_i, \tag{4.1}$$

where J_i is the appropriate expression for homogeneous nucleation of component i. For case (1) above, Eq. (4.1) goes as

$$J_B \approx (1 - x^*)^{1/2}(2\pi n_2^*)^{1/2} J_2, \tag{4.2}$$

and for case (2) as

$$J_B \approx (x^*)^{1/2}(2\pi n_1^*)^{1/2} J_1. \tag{4.3}$$

These expressions clearly approach zero under the above limiting conditions. Thus, although the correct limiting behavior is found for the thermodynamic aspects of the theory, taking into account the proper form for the equilibrium distribution, the kinetic prefactor is seen to be inconsistent with physical expectations.

The basis of the difficulty can be traced to Reiss' definition of the nucleation rate, Eq. (2.15), because until

its final stage of development the binary kinetics scheme does reduce correctly to homogeneous nucleation under the appropriate conditions. Implicit in the definition of the rate is the assumption that the pass is broad enough so that a large number of currents make a significant contribution to the over-all nucleation rate. If the steady state problem were solved without treating the n_i as continuous, the overall rate would be the discrete sum of those currents which lead to the formation of clusters whose composition is such as to allow growth into larger fragments of the new phase. Most of these currents would undoubtedly be bunched about the saddle point composition.

Since the problem is much more tractable in the continuous approximation, the sum is taken to be given approximately as the integral of the current over the pass-width with the limits of integration of $\pm\infty$ used for convenience. For conditions under which it is invalid to convert the sum into an integral, Eq. (2.15) will prove inadequate. Such conditions arise for the limiting cases that were discussed.

What happens is simply that, in the limit, the free energy surface becomes singular for all cluster compositions except those on the path of homogeneous nucleation for the appropriate species. This behavior is manifested in the divergence of q [Eq. (2.21b)], the curvature of w in the direction perpendicular to the pass axis. The function $I(\xi_2)$ vanishes unless $\xi_2 = 0$ (homogeneous nucleation), and its integral likewise vanishes. From the discrete point of view, what happens is that, in the limit, the addition of only one molecule of the inappropriate species to the previously pure cluster results in a tremendous increase in the free energy of formation. Thus, the free energy surface exhibits a large stepwise discontinuity. It is finite and well behaved on the path of homogeneous nucleation, but not elsewhere. The sum that defines the rate now collapses to a single term, that expected for homogeneous nucleation. The divergence of q is now seen to be a consequence of the continuous approximation.

In order to preserve the convenience of the continuous approximation without incurring the demonstrated consequences of its failure, what is needed is a simple technique for interpolating between the regions where only homogeneous nucleation is significant and those where Eq. (2.15) is an acceptable definition of the rate. The following *ad hoc* proposal, though inelegant, ought to be satisfactory. The rate is defined as

$$J_B = \frac{\nu(\Delta l)}{2\Delta l} \int_{-\Delta l}^{\Delta l} I(\xi_2) d\xi_2 , \tag{4.4}$$

where $I(\xi_2)$ is still given by Eq. (2.11) or (2.13) and ν Δl are related to the width of the pass in a manner to be prescribed shortly. This equation can be interpreted as the average nucleation current per unit length (of pass-width) flowing through the pass multiplied by the function $\nu(\Delta l)$ which counts the total number of currents contributing to the over-all rate.

For a broad pass, Δl may be taken large enough so that agreement of Eq. (4.4) with Eq. (2.15) may be obtained by letting $\nu(\Delta l) \approx 2\Delta l$. Geometric considerations show this to be a suitable approximation. As the pass narrows, this agreement is not permitted. Instead, the following behavior pertains.

First, since there will always be at least one current contributing to the rate (provided one of the components is supersaturated), the function ν must never be less than unity even as $\Delta l \to 0$. In practice, ν will reach this limiting value long before Δl approaches zero and will then remain constant. Now Eq. (4.4) may be formally rewritten as

$$J_B = \nu(\Delta l) \int_{-\infty}^{\infty} d\xi_2 I(\xi_2) \left\{ \frac{H(\xi_2 + \Delta l) - H(\xi_2 - \Delta l)}{2\Delta l} \right\}, \tag{4.5}$$

where $H(x)$ is the Heaviside step function and is equal to one when x is positive and is zero otherwise. Recalling that the Dirac delta function $\delta(x)$ is the derivative of $H(x)$, Eq. (4.5) yields, as $\Delta l \to 0$,

$$J_B = \int_{-\infty}^{\infty} d\xi_2 I(\xi_2) \delta(\xi_2) \tag{4.6}$$

or

$$J_B = I(0) . \tag{4.7}$$

Consideration of Eqs. (4.4) and (2.18) shows that this result is well defined provided $\Delta l \to 0$ faster than $q^{1/2} \to \infty$, and it is precisely the desired result, since the other terms in the prefactor go over smoothly to the homogeneous nucleation limit.

The function ν poses no computational problems, but in order to use Eq. (4.4) a prescription for Δl must be supplied. As the saddle point approaches either the n_1 or n_2 axis, a convenient choice for Δl is the length of a line perpendicular to the axis of the pass originating at the saddle point and ending at whichever axis is being approached. As the n_1 axis is approached, some trigonometric considerations give

$$\Delta l = n_2^* / \cos\phi . \tag{4.8}$$

Similarly, as the n_2 axis is approached,

$$\Delta l = n_1^* / \sin\phi . \tag{4.9}$$

Consideration of the limiting behavior of q from Appendix B leads immediately to the conclusion that $\Delta l (q)^{1/2} \to 0$ as either axis is approached. These choices for Δl are thus consistent with the required limiting procedure.

With Eq. (2.14), Eq. (4.4) can be rewritten as

$$J_B = J(n_1^*, n_2^*) \frac{\nu(\Delta l)}{2\Delta l} \operatorname{erf}[\Delta l (q/2kT)^{1/2}], \tag{4.10}$$

where

$$J(n_1^*, n_2^*) = D^* (p/q)^{1/2} c(n_1^*, n_2^*), \tag{4.11}$$

$$p = -\left(\frac{\partial^2 \ln c}{\partial \xi_1^2} \right)^* , \tag{4.12a}$$

$$q = \left(\frac{\partial^2 \ln c}{\partial \xi_2^2} \right)^* , \tag{4.12b}$$

and

$$\operatorname{erf}(x) = (2/\sqrt{\pi}) \int_0^x e^{-v^2} dv . \tag{4.13}$$

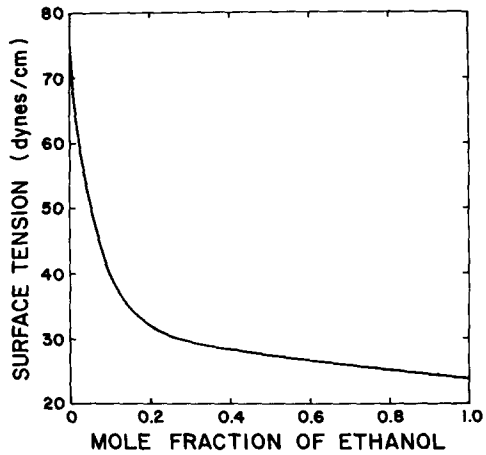

FIG. 1. Surface tension of the ethanol–water system at 273 °K.

Equation (4.10) has the form of Reiss' result multiplied by a correction factor which becomes important only when the pass is narrow.

V. RESULTS FOR THE ETHANOL–WATER SYSTEM

Published experimental data on homogeneous nucleation in binary vapors can apparently be found only in the pioneering work of Flood[15]; however, Kaser[16] has mentioned that these experiments may involve nucleation on ions. Additionally, some qualitative results have been reported,[17] and some unpublished work exists.[18] All of these experiments deal with the ethanol–water system, and for that reason so do the present calculations which were made using the rate expressions given by Eqs. (2.19) and (4.10). It should be noted that no provision was made for including statistical mechanical effects in the calculations; in other words, only Eq. (2.3) was used for the equilibrium distribution.

In order to perform the calculations, the surface tension, density, and equilibrium vapor pressure of water and ethanol are needed as functions of solution composition and temperature. Values of the surface tension[19] at 14 different compositions were fitted to either first or second order polynomials as functions of $T(°K)$ with an accuracy of usually much better than 0.5%. These σ vs T curves were then used to generate "data" points at any specified temperature as a function of mole fraction, x. Fitting $\ln(\sigma)$ vs a third order polynomial in the variable $4x/(1+3x)$ gave a reproducibility of better than 0.5%. In Fig. 1, the surface tension of the ethanol–water mixture at 273 °K is presented. Quadratic curves of the density ρ vs T were obtained from data[20] at 21 different mass fractions with an accuracy usually better than 0.01%. These curves were used to generate density values at specified temperatures which could be fitted to a second order polynomial as a function of the mass fraction with an accuracy of about 0.1%. The partial and average molecular volumes were computed as functions of composition using these fitted density curves.

Vapor pressure data[21] at 293 and 313 °K (following Flood) were fitted to straight lines. These curves were used in a fashion similar to that above with the following exceptions. Below 280 °K, the vapor pressure of pure ethanol was calculated using the equation of Wegener, Clumpner, and Wu.[17] The vapor pressure of water was always computed using the equation of Keenan and Keyes.[22] For the temperature range used in these calculations, these values agreed well with data compiled in the *Handbook of Chemistry and Physics*.[23] For mole fractions of ethanol less than 0.089 and greater than 0.95, Raoult's law was used to generate data points for, respectively, the water and ethanol equilibrium vapor pressure curves. These points were used as input to the fitting program in the place of the (ostensibly inaccurate) points extrapolated from the values in the *International Critical Tables*.[21]

It was found that the vapor pressure data at 273 and 280 °K could be fitted with an error of usually less than 2% to a third or fourth order polynomial in a variable z, where $z = x[0.8(x-0.75)^2 + 0.95]$ for water and $z = x[2.5 \times (x-0.8)^2 + 0.9]$ for ethanol. This accuracy is acceptable because a 1 °K change in temperature at 273 °K produces roughly a 9% change in the vapor pressures. However, since these fitted curves did not possess zero intercepts (partial vapor pressure must vanish when a component is absent), Henry's law was invoked for the low concentration species whenever Raoult's law was applicable for the other component. The appearance of these vapor pressure curves, shown in Fig. 2, is qualitatively correct, but in the absence of experimental data there is no quantitative way to judge accuracy.

To illustrate the effects of real solution behavior, calculations were also performed for an *ideal* ethanol–water system. Here, surface tension and density were identical with the real system, but vapor pressures were given simply by Raoult's law over the entire composition range.

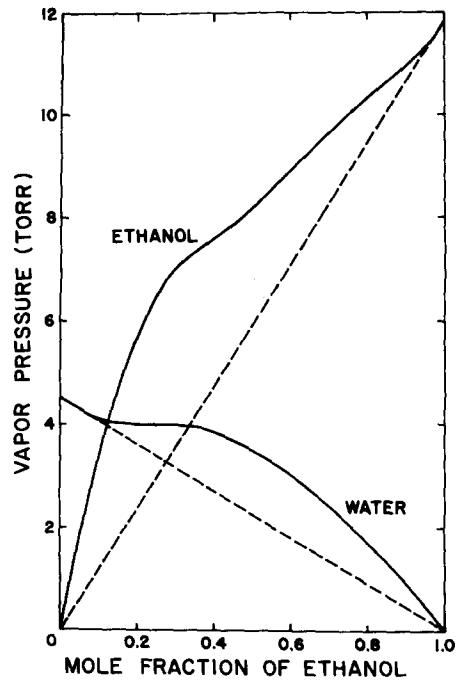

FIG. 2. Equilibrium vapor pressure curves for the ethanol–water system at 273 °K.

TABLE I. Experimental critical activities calculated from Flood's[15] data. Components 1 and 2 are water and ethanol, respectively. The equilibrium vapor pressure of pure substance i is denoted p_i^0; a_i is the activity of component i. The initial and final temperatures carry the subscripts i and f. The solution composition is given in terms of the mole fraction of ethanol, y. The p_i^s are the partial vapor pressures of a solution of composition y, and E is Flood's volume expansion ratio.

y	E	T_i(°K)	$p_1^s(y)$ (Torr)	$p_2^s(y)$ (Torr)	T_f(°K)	p_1^0 (Torr)	p_2^0 (Torr)	a_1	a_2
0.039	1.155	291	14.72	5.36	272.8	4.47	11.7	2.67	0.37
0.115	1.115	289	12.11	11.30	275.6	5.47	14.4	1.89	0.67
0.353	1.101	292	13.27	23.66	280.4	7.64	20.1	1.51	1.03
0.671	1.114	289.8	7.20	28.13	277.	6.04	15.9	1.02	1.52
0.779	1.119	288	5.38	26.47	274.9	5.20	13.6	0.88	1.66
0.903	1.142	289	2.64	31.14	273.8	4.81	12.60	0.45	2.05

In addition to calculating the nucleation rate as a function of the partial pressures of the components, critical activity curves for the onset of condensation were also computed. Assuming ideal gas behavior, the activity is the ratio of the partial pressure of the vapor to its equilibrium vapor pressure over pure liquid. Critical activities are those values for which the rate of binary nucleation is just equal to some prespecified value.

In order to compare Flood's results with these calculations, the experimental critical activities must be calculated from his results. This requires knowledge of the equilibrium vapor pressures of the solutions at his starting temperatures. Since there is no need to be able to calculate $p^s(x)$ for any composition, polynomial fits were not tried. Instead, it was much simpler to use linear interpolation between the appropriate pair of data points calculated at the desired temperature. Then, using Flood's second unnumbered equation on p. 289 and his reported values for E, T_1, T_2, and solution composition, the critical activities may be calculated. These are listed in Table I and are also presented in Fig. 3, where the calculated curves are shown. For the $J_B = 1$ (cc-sec)$^{-1}$ curve at 273 °K, quantities characterizing the saddle point are listed in Table II. Quantitative agreement is fair to poor, with the largest discrepancies arising for larger values of water vapor activity. There is a clear need for further experiments and theory to resolve this issue.

The real solution effects apparent in Figs. 3 and 4 are easy to explain. For given activities, the effective supersaturations achieved in the real system are usually significantly lower than those of the ideal system because of the positive deviation from ideality of the vapor pressure curves. The lower supersaturations necessitate either lower rates or higher activities to achieve a given rate.

For the activity ranges studied, use of the modified Reiss theory did not change the calculated activity curves. However, in Fig. 4 it may be seen that rates calculated with these different equations show a clear divergence as the activity of water vapor is reduced. While the conditions under which this divergence occurs may border on the extreme for this example, it still seems desirable to have a rate equation which properly yields homogeneous nucleation when the physical conditions so dictate. Such behavior will be useful, for example, when evaluating data for experiments involving trace amounts of condensibles or when trying to include statistical mechanical corrections to the rate equation in a manner consistent for both binary and homogeneous nucleation. It unfortunately appears that such a rate expression cannot be obtained unless the full time dependence of the nucleation process is included. The basis for this remark will be discussed below and in Sec. VI.

Numerical studies of the limiting behavior of the rate equations for vanishing amounts of ethanol vapor uncovered the following behavior. Even for an ethanol activity as ridiculously low as 10^{-10} and a water activity of 9, the 24 molecule cluster still contained 1.7% ethanol. The explanation of this drastic behavior is simple. The surface tension of pure water is so high (see Fig. 1) that the tendency to resist the formation of pure water clusters is very great. Numerically, *x was found* to decrease as

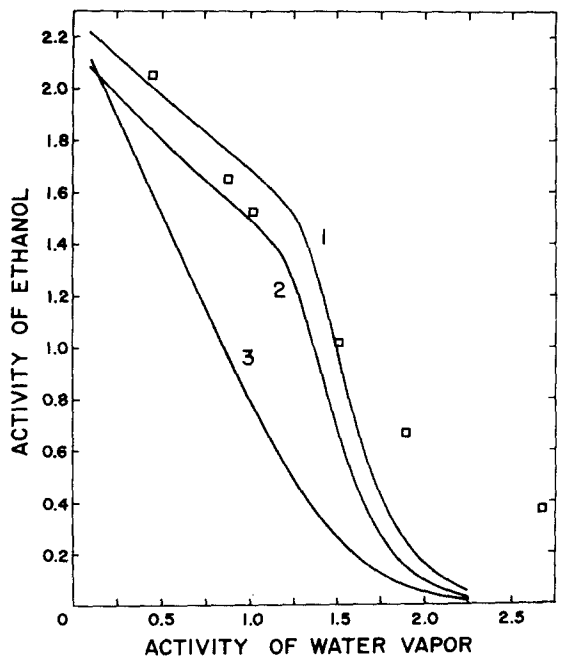

FIG. 3. Critical activity curves for the onset of condensation in the ethanol–water system for a nucleation rate of 1 (cc – sec)$^{-1}$ at 273 °K, Curve 1, and at 280 °K, Curve 2. Flood's experimental results are marked by □. Also shown is the onset curve at 273 °K [$J_B = 1$ (cc-sec)$^{-1}$], Curve 3, for the ideal ethanol–water system discussed in Sec. V.

TABLE II. Quantities characterizing the saddle point for $J_B = 1$ (cc-sec)$^{-1}$ at 273 °K. Components 1 and 2 are water and ethanol, respectively. The frequency factor K is defined as $K = J_B \exp(w^*/kT)$; p_i^0 is the equilibrium vapor pressure of pure component i; $p_1^0 = 4.54$ Torr, $p_2^0 = 11.8$ Torr.

p_1/p_1^0	p_2/p_2^0	x	$S_1(x)$	$S_2(x)$	r^*(Å)	$n_1^* + n_2^*$	w^*/kT	K (cc − sec)$^{-1}$ (×10^{26})
0.1	2.21	0.965	1.52	2.26	14.96	151.9	60.82	2.60
0.5	1.97	0.830	1.51	2.25	14.83	164.9	61.37	4.48
0.6	1.92	0.795	1.51	2.25	14.79	168.4	61.45	4.89
0.75	1.83	0.736	1.51	2.25	14.71	174.6	61.60	5.65
0.85	1.77	0.692	1.51	2.25	14.64	179.5	61.71	6.29
1.0	1.69	0.615	1.51	2.24	14.52	188.6	61.86	7.35
1.2	1.56	0.478	1.53	2.22	14.22	204.6	61.76	6.64
1.4	1.24	0.312	1.62	2.05	13.61	219.0	60.73	2.37
1.6	0.72	0.203	1.80	1.50	12.89	216.2	59.63	0.787
1.8	0.35	0.148	2.01	0.911	12.30	203.6	58.94	0.396
2.0	0.15	0.116	2.21	0.487	11.81	189.7	58.53	0.263
2.25	0.049	0.0896	2.46	0.192	11.31	173.5	58.23	0.194

the ethanol activity decreased; but because of the magnitude of σ and $d\sigma/dx$, the region displaying the limiting behavior discussed in the Appendices was never reached. Under these circumstances, both rate equations behaved as Eq. (6.1), and the predicted rate ultimately dropped well below that of homogeneous nucleation of water, which now became, by far, the largest contribution to the overall nucleation rate of the system.

VI. DISCUSSION

As noted, there are circumstances for which both definitions of the nucleation rate will fail to provide a qualitatively correct estimate. In any binary system, some homogeneous nucleation will be taking place unless the components are undersaturated with respect to the vapor pressure of the pure liquid. Because the steady state rate of mixed cluster formation is normally much higher than that of pure cluster formation, neglecting the latter rate is usually not serious. In systems for which thermodynamic properties are appropriate, it may be possible to significantly lower the vapor concentration of one of the components without necessitating, on thermodynamic grounds, the formation of pure or nearly pure clusters of the more abundant species. That is, the pressure is low, but not so low that the limiting behavior discussed in the Appendices is reached.

For instance, suppose $p_1 \gg p_2$. Then Eq. (4.10) behaves as

$$J_B \approx \frac{\beta_2 \mathcal{O}^*}{\sin^2\phi} (p/q)^{1/2} c(n_1^*, n_2^*), \tag{6.1}$$

and the steady state rate will be limited by the vapor concentration of the less abundant species. Possibly, because of the lower free energy of mixed cluster formation, this rate will still be higher than that of homogeneous nucleation of Species 1. Even so, it is entirely possible that the time lag needed for the attainment of this rate is much longer than that needed to attain steady state nucleation of Species 1 alone. Thus, on kinetic grounds, homogeneous nucleation of component 1 would be the predominant rate process taking place, but its contribution, under these circumstances, is not included in either definition of the rate and must be calculated independently. A more elaborate discussion of the role of time lags in binary nucleation will be provided in the following paper.

Another remark is somewhat speculative. Even if the saddle point is not too close to either the n_1 or n_2 axis, there may be some peculiar thermodynamic property of the system of interest which permits only a single unique path for nucleation, i.e., the pass becomes a very narrow crevice, but in the interior region, not on the axis. Possible causes of such behavior are, for example, a deep minimum in the surface tension over a small composition range or the onset of (partial) immiscibility. In such cases, an equation like Eq. (4.10) will be the preferred definition of the rate.

Other effects may also be important. For example, Heist and Reiss[24] have considered hydrate formation in binary sulfuric acid–water vapor, and Hirschfelder[25] has extended Reiss' theory to multicomponent systems. Finally, Stauffer, Binder, and Wildpaner[26] have recently considered the effects of surface enrichment in binary clusters.

Note added in proof: New considerations,[27] which appeared after this article had been submitted, may provide a more satisfactory rate expression in the transition regions near the n_1 and n_2 axes than the *ad hoc* proposal made in Sec. IV.

ACKNOWLEDGMENTS

I am deeply indebted to Professor P. P. Wegener for his support and encouragement. I benefited greatly from conversations with Professor W. J. Dunning and Professor J. L. Katz and Dr. P. Mirabel and Dr. B. J. C. Wu. I would also like to thank Dr. P. Merkli for helping me understand Flood's article. Finally, I must thank Don, Lorrie, and Mojmir for their aid in my struggle with Grendel.

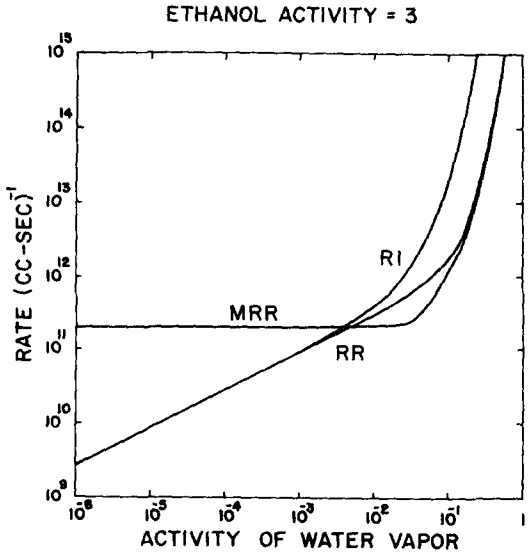

FIG. 4. Binary nucleation rates calculated at an ethanol activity of 3 as a function of water vapor activity; $T = 273$ °K. Curves depicted: RR, Reiss theory for the real system; MRR, modified Reiss theory for the real system; RI, Reiss theory for the ideal system.

APPENDIX A: LIMITING BEHAVIOR OF THE GIBBS–THOMSON EQUATIONS

The equations of concern are Eqs. (2.7). First consideration will be given to the case for which $p_1 \to 0$ or $p_1^s(x) \to \infty\ (x \neq 1)$. Restrict consideration to the neighborhood of $x = 1$. It will always be possible to pick pressures to meet this restriction. In this region, Henry's law may be used for $p_1^s(x)$,

$$p_1^s(x) = (1-x)K_1 . \tag{A1}$$

Define a parameter κ_1, where $\kappa_1 = p_1/K_1$. Then both limits may be investigated simultaneously by considering the limit $\kappa_1 \to 0$. Next rewrite Eq. (2.7a) as

$$kT \ln[\kappa_1/(1-x)] = U_1(x), \tag{A2}$$

where

$$U_1(x) = r^{-1}\left(2\sigma v_1 - 3xv\frac{d\sigma}{dx}\right). \tag{A3}$$

Depending on the sign and magnitude of $d\sigma/dx$, $U_1(1)$ can be positive, negative, or zero. However, barring severely pathological behavior, $U_1(x)$ will approach $U_1(1)$ monotonically. Two cases arise.

(1) If $U_1(x) > 0$ in this region, then

$$\kappa_1/(1-x) > 1 \tag{A4}$$

in order to satisfy Eq. (A2). As $\kappa_1 \to 0$, then, necessarily $x \to 1$ to satisfy Eq. (A4). Also note that $\Delta\mu_1(x)$ has a well defined value for this double limit, namely

$$\lim_{\substack{\kappa_1 \to 0 \\ x \to 1}} \Delta\mu_1 = -U_1(1). \tag{A5}$$

(2) If $U_1(x) < 0$ in this region, then

$$\kappa_1/(1-x) < 1 \tag{A6}$$

to satisfy Eq. (A2). As $\kappa_1 \to 0$, it is necessary that $x \to 1$, in accordance with the inequality of Eq. (A6) if both sides of Eq. (A2) are to be well defined. Note that Eq. (A6) implies that Species 1 can be *undersaturated* with respect to its vapor pressure over a bulk solution of composition x (cf. the bottom entries of Table II). The explanation of this unusual behavior may be that the chemical potential of Species 1 in the droplet, as compared to that in bulk solution, receives an extra contribution from the composition dependence of the surface tension, which can become very significant. Alternatively, this behavior may just be an artifact arising because surface enrichment effects[26] were not considered.

A restriction on the solutions of Eq. (2.7) comes if these equations are solved for r (really r^*):

$$r = \frac{-2\sigma v}{(1-x)\Delta\mu_1 + x\Delta\mu_2} . \tag{A7}$$

Since $r > 0$, Eq. (A7) restricts the amount any one component can be undersaturated (relative to the bulk solution) if nucleation is to take place at all.

Lastly, note as $x \to 1$, Eq. (2.7b) becomes

$$\Delta\mu_2 = \frac{-2\sigma v_2}{r} , \tag{A8}$$

the usual Gibbs–Thomson equation for a pure droplet.

Analogous behavior can be deduced from Eq. (2.7b) as $p_2 \to 0$ or $p_2^s(x) \to \infty\ (x \neq 0)$, with the results

$$x \to 0,$$

$$\lim_{\substack{\kappa_2 \to 0 \\ x \to 0}} \Delta\mu_2 = -U_2(0), \tag{A9}$$

where

$$U_2(x) = r^{-1}\left(2\sigma v_2 + 3v(1-x)\frac{d\sigma}{dx}\right), \tag{A10}$$

and from Eq. (2.7a),

$$\Delta\mu_1 = -2\sigma v_1/r . \tag{A11}$$

APPENDIX B: LIMITING BEHAVIOR OF THE KINETIC PREFACTOR

When inconvenient, the superscript * will not be used; however, all quantities are assumed to be evaluated at the saddle point.

To analyze the limiting behavior of the prefactor of Eq. (2.19), i.e., $D^*(p/q)^{1/2}$, the asymptotic behavior of ϕ, p, and q is needed.

Equations (2.21) yield

$$-p = \cos^2\phi\,\frac{\partial^2 w}{\partial n_1^2} + 2\cos\phi\,\sin\phi\,\frac{\partial^2 w}{\partial n_1 \partial n_2} + \sin^2\phi\,\frac{\partial^2 w}{\partial n_2^2} , \tag{B1}$$

$$q = \sin^2\phi\,\frac{\partial^2 w}{\partial n_1^2} - 2\cos\phi\,\sin\phi\,\frac{\partial^2 w}{\partial n_1 \partial n_2} + \cos^2\phi\,\frac{\partial^2 w}{\partial n_2^2} . \tag{B2}$$

The angle ϕ may be calculated from the relation[2]

$$\tan 2\phi = \frac{2(\partial^2 w/\partial n_1 \partial n_2)}{(\partial^2 w/\partial n_1^2) - (\partial^2 w/\partial n_2^2)} . \tag{B3}$$

This equation is also satisfied by $\phi + \pi/2$, so appropriate care must be taken to insure that the proper branch of the function is being calculated. Equations (2.5) and (2.8) and the relation

$$4\pi r^3/3 = (n_1 + n_2)v \tag{B4}$$

will prove useful in simplifying the various expressions that will be obtained.

Consider first what happens as $x^* \to 1$. Straightforward calculation of $\partial^2 w/\partial n_1 \partial n_2$ gives an expression which can be simplified by using Eqs. (B4), (2.5), and (2.8), assuming that $\partial v_1/\partial x$ and $\partial\sigma/\partial x$ are not infinite at $x = 1$ and that $\sigma(x)$ is only a function of x and not of the total number of molecules in the cluster. The results at $x = 1$ $(n_1^* = 0)$ is

$$\frac{\partial^2 w}{\partial n_1 \partial n_2} = \frac{\partial \Delta\mu_1}{\partial n_2} - \frac{v_2}{r}\left(\frac{2v_1\sigma}{4\pi r^3} + \frac{d\sigma}{dn_1}\right). \tag{B5}$$

In similar fashion, the remaining derivatives may be calculated. Near $x = 1$, Henry's law

$$p_1^s(x) = (1-x)K_1 , \tag{B6}$$

and Raoult's law

$$p_2^s(x) = x p_2^s(1), \tag{B7}$$

may be employed in order to evaluate the derivatives of the $\Delta\mu_i$. Upon doing so, and using Eq. (A5), the follow-

ing results are obtained:

$$\left.\frac{\partial^2 w}{\partial n_1 \partial n_2}\right|_{x=1} = -\frac{kT}{n_2^*} + \frac{U_1(1)}{3n_2^*}, \tag{B8}$$

$$\frac{\partial^2 w}{\partial n_1^2} \approx \frac{1}{1-x^*}\,\frac{kT}{n_2^*}, \tag{B9}$$

$$\left.\frac{\partial^2 w}{\partial n_2^2}\right|_{x=1} = \frac{\Delta\mu_2(x=1)}{3n_2^*}. \tag{B10}$$

Equations (B3) and (B8)–(B10) imply

$$\tan 2\phi \approx -2(1-x^*)\left|1+\frac{U_1(1)}{3n_2^*}\right|. \tag{B11}$$

Absolute value signs have been used to insure that ϕ is really the angle of orientation of the pass *axis*.

From Eq. (B11), it is easy to deduce that

$$\sin^2\phi \approx 1, \tag{B12}$$

$$\cos^2\phi \approx (1-x^*)^2\left(1+\frac{U_1(1)}{3n_2^*}\right)^2. \tag{B13}$$

Then, Eqs. (B1), (B2), (B8)–(B10), (B12), and (B13) imply

$$p = -\frac{\Delta\mu_2(x=1)}{3n_2^*}, \tag{B14}$$

$$q \approx \frac{1}{1-x^*}\,\frac{kT}{n_2^*}, \tag{B15}$$

$$D^*(p/q)^{1/2} \approx (1-x^*)^{1/2}(2\pi n_2^*)^{1/2}\left[\beta_2 \mathcal{O}^*\left(\frac{-\Delta\mu_2(x=1)}{6\pi n_2^* kT}\right)^{1/2}\right]. \tag{B16}$$

At the other extreme, $x^* \to 0$, the following results may readily be obtained:

$$\left.\frac{\partial^2 w}{\partial n_1 \partial n_2}\right|_{x=0} = -\frac{kT}{n_1^*} - \frac{U_2(0)}{3n_1^*}, \tag{B17}$$

$$\left.\frac{\partial^2 w}{\partial n_1^2}\right|_{x=0} = \frac{\Delta\mu_1(x=0)}{3n_1^*}, \tag{B18}$$

$$\frac{\partial^2 w}{\partial n_2^2} \approx \frac{1}{x^*}\,\frac{kT}{n_1^*}. \tag{B19}$$

From these it follows that

$$\tan 2\phi \approx 2x^*\left|1+\frac{U_2(0)}{3kT}\right|, \tag{B20}$$

$$\sin^2\phi \approx (x^*)^2\left(1+\frac{U_2(0)}{3kT}\right)^2, \tag{B21}$$

$$\cos^2\phi = 1. \tag{B22}$$

Finally,

$$p = -\frac{\Delta\mu_1(x=0)}{3n_1^*}, \tag{B23}$$

$$q \approx \frac{1}{x^*}\,\frac{kT}{n_1^*}, \tag{B24}$$

and

$$D^*(p/q)^{1/2} \approx (x^*)^{1/2}(2\pi n_1^*)^{1/2}\left[\beta_1 \mathcal{O}^*\left(\frac{-\Delta\mu_1(x=0)}{6\pi n_1^* kT}\right)^{1/2}\right]. \tag{B25}$$

*The support of the Power Program of the Office of Naval Research is gratefully acknowledged.

†Present address: Department of Chemistry, Dartmouth College, Hanover, New Hampshire 03755.

[1]H. Reiss, J. Chem. Phys. **18**, 840 (1950).
[2]G. J. Doyle, J. Chem. Phys. **35**, 795 (1961).
[3]C. S. Kiang and D. Stauffer, in *Faraday Symposia of the Chemical Society*, No. 7, 26 (1973). D. Stauffer and C. S. Kiang, Icarus **21**, 129 (1974), and other references cited therein.
[4]R. A. Sigsbee, in *Nucleation*, edited by A. C. Zettlemoyer (Marcel Dekker, New York, 1969), Chap. 4.
[5]P. Mirabel and J. L. Katz, J. Chem. Phys. **60**, 1138 (1974).
[6]W. J. Dunning, in *Nucleation*, edited by A. C. Zettlemoyer (Marcel Dekker, New York, 1969), Chap. 1.
[7]M. Blander and J. L. Katz, J. Stat. Phys. **4**, 55 (1972).
[8]P. M. Morse and H. Feshbach, *Methods of Theoretical Physics* (McGraw-Hill, New York, 1953), Vol. I, pp. 21–32.
[9]J. L. Katz (private communication, 1973).
[10]D. Barschdorff, W. J. Dunning, B. J. C. Wu, and P. P. Wegener, Nat. Phys. Sci. **240**, 166 (1972).
[11]J. Feder, K. C. Russell, J. Lothe, and G. M. Pound, Adv. Phys. **15**, 111 (1966).
[12]P. P. Wegener and J.-Y. Parlange, Naturwissenschaften **57**, 525 (1970).
[13]*Nucleation*, edited by A. C. Zettlemoyer, (Marcel Dekker, New York, 1969). See the first three chapters in particular.
[14]W. J. Dunning (private communication, 1972). This result differs by a factor of n from that described in Ref. 6.
[15]H. Flood, Z. Phys. Chem. A **170**, 286 (1934). Note that droplet compositions calculated by Flood are in error, as pointed out by Mirabel and Katz.[5] This error is evidently reproduced in Kaser's[16] summary of Flood's work.
[16]A. Kaser, Z. Angew. Math. Mech. **53**, 39 (1973).
[17]P. P. Wegener, J. A. Clumpner, and B. J. C. Wu, Phys. Fluids **15**, 1869 (1972).
[18]J. A. Clumpner, Ph.D. thesis, Yale University, 1970; B. J. C. Wu and K. C. Belle, Bull. Am. Phys. Soc. **19**, 1150 (1974).
[19]B. Y. Teitelbaum, T. A. Gortalova, and E. E. Siderova, Zh. Fiz. Khim. **25**, 911 (1951); as recorded in J. Timmermans, *Physico-Chemical Constants of Binary Systems* (Interscience, New York, 1960), Vol. 4, p. 197.
[20]W. Kreitling, thesis, Erlangen, 1892; as recorded in J. Timmermans, *Physico-Chemical Constants of Binary Systems*, (Interscience, New York, 1960), Vol. 4, p. 184.
[21]*International Critical Tables* (McGraw-Hill, New York, 1928), Vol. III, p. 290.
[22]J. H. Keenan and F. G. Keyes, *Thermodynamic Properties of Steam* (Wiley, New York, 1936), Eq. (12).
[23]*Handbook of Chemistry and Physics*, edited by R. C. Weast, (The Chemical Rubber Co., Cleveland, Ohio, 1970–71), 51 ed.
[24]R. H. Heist and H. Reiss, J. Chem. Phys. **61**, 573 (1973).
[25]J. O. Hirschfelder, J. Chem. Phys. **61**, 2690 (1974).
[26]D. Stauffer, K. Binder, and V. Wildpaner, Water, Air, and Soil Pollution **3**, 515 (1974).
[27]W. J. Shugard, R. H. Heist, and H. Reiss, J. Chem. Phys. **61**, 5298 (1974).